

# BEAM LOSS STUDY FOR THE IMPLEMENTATION OF DECHIRPER AT THE EUROPEAN XFEL

J. J. Guo<sup>1\*</sup>, University of Chinese Academy of Sciences, Beijing, China  
W. Decking, M. Guetg, S. Liu<sup>†</sup>, W. L. Qin, I. Zagorodnov, DESY, Hamburg, Germany  
Q. Gu<sup>1</sup>, SARI, Shanghai, China  
<sup>1</sup>also at SINAP, Shanghai, China

## Abstract

The European XFEL is a free-electron laser facility based on superconducting linac with high repetition rate up to 4.5 MHz. Wakefield structure (also called dechirper module) is planned to be installed in front of the SASE beam line at the European FEL, which can be used as a kicker for two-color scheme or a dechirper to control the bandwidth of SASE radiation. When the beam pass through the dechirper module, strong longitudinal and transverse wakefields can be excited to introduce a correlated energy chirp and a kick along the bunch. However, due to the relatively small gap of dechirper, beam halo particles hitting the dechirper module can lead to energy deposition and generate additional radiation, which can cause serious damage to the downstream undulators. For this reason, simulations have been performed using BDSIM to define the maximum acceptable beam halo, and the results are presented in this paper.

## INTRODUCTION

The European XFEL is designed to be operated with beam energy up to 17.5 GeV with 10 Hz pulsed mode carrying a maximum of 2700 bunches per macro pulse [1]. The high beam power 500 kW together with the high loss sensitivity of the undulators raises serious radiation damage concern. This concern is a common issue for all high power machines (e.g. LCLS-II [2], SHINE [3]).

The dechirper module, also called wakefield structure, is capable of manipulating the electron beam longitudinal and transverse phase space to tailor the FEL performance in temporal and/or frequency domain. The longitudinal wakefield introduces a correlated energy chirp along the bunch which can be used to increase or to decrease the radiation bandwidth of SASE, and the transverse dipole wakefield introduces a correlated kick along the bunch which can be used for beam diagnostics or fresh-slice lasing schemes. Successful experiments using the RadiaBeam dechirper as a fast kicker for fresh-slice applications have been demonstrated at the LCLS [4–6] with low repetition rate.

At European XFEL with high repetition rate, a dechirper device to be placed upstream of SASE1 undulator is being investigated for fresh-slice applications. Despite the above mentioned benefits of the dechirper, due to the high beam power and the small gap of the dechirper, large beam losses can be produced when a beam with large beam halo extension passes through the dechirper. Secondary particles

generated in this process may be transmitted downstream and cause radiation damage to the downstream undulators. Therefore evaluation of the beam loss and radiation dose is crucial for the implementation of the dechirper. In this paper, beam loss simulations using beam halo with extension up to different number of beam size sigmas have been performed using BDSIM code [7].

## THE LOCATION AND GEOMETRY OF DECHIRPER STRUCTURE

In the simulation, two dechirper modules are located upstream of SASE1 and downstream of SASE2 distribution kickers, as indicated by the red arrow in Fig. 1 below. The geometry of the dechirper module is shown in Fig. 2, where the dechirper module is horizontally oriented. Detailed parameters of the dechirper module are listed in Table 1, which are taken from Reference [8].

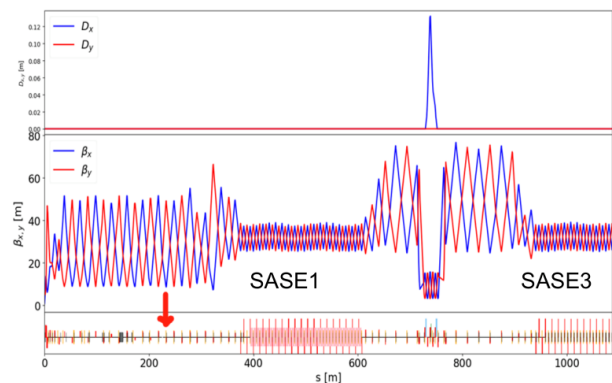


Figure 1: The design optics along SASE1 and SASE3, and the position of dechirper. The red arrow points to the position of dechirper.

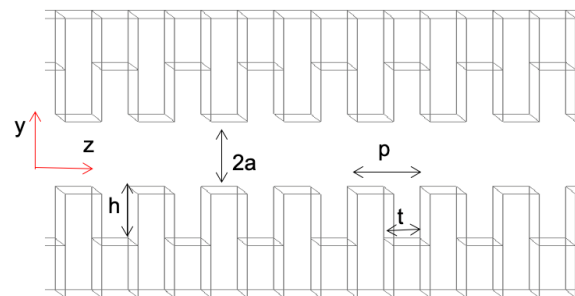


Figure 2: Geometry of the dechirper module.

\* junjie.guo@desy.de, guojunjie@sinap.ac.cn  
<sup>†</sup> shan.liu@desy.de

Table 1: Parameters of One Dechirper Module

Parameter Name	Value (mm)
Depth, h	0.5
Gap, t	0.25
Period, p	0.5
Half aperture, a	0.7
Half width, w	6
Length, L	2000

## SIMULATION MODEL

The model used in the simulations is depicted in Fig. 3, which starts from the dechirper element and includes downstream transport line quadrupoles to SASE1, SASE1 undulators and the undulator quadrupoles in the intersections. The vacuum chambers with two chamber aperture transitions are also included in the model: first from  $\phi 40.5$  mm to  $\phi 10$  mm followed by the elliptical undulator vacuum chamber with semi-major axis length of 7.5 mm and semi-minor axis length of 4.4 mm. Electron beam parameter settings used in the simulation are listed in Table 2. The beam halo is generated from BDSIM [9] with a flat distribution in phase space and it only starts from 10 beam size sigma up to different number of sigmas (15 sigma to 20 sigma) to increase the statistics.

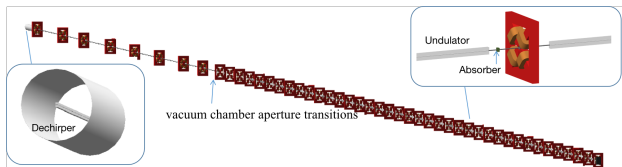


Figure 3: Geometry from dechirper to SASE1 used in the BDSIM simulation.

Table 2: Beam Parameters Used in Simulations

Parameter Name	Value	Unit
Beam energy, E	14	GeV
Alpha function, $\alpha_x/\alpha_y$	1.25/-1.67	
Beta function, $\beta_x/\beta_y$	19.93/27.56	m
Emittance, $\epsilon_x/\epsilon_y$	0.64/1.09	$\mu\text{m}$
Number of primary particle, N	$4 \times 10^6$	
Beam halo start sigma, $\sigma$	$\pm 10$	
Beam halo stop sigma, $\sigma$	$\pm(15-20)$	

## ENERGY DEPOSITION AND RADIATION DOSE

In our simulation, a total number of  $4 \times 10^6$  electrons with different number of sigmas were generated to transport through the dechirper module, and the energy losses were recorded. The energy loss map from the dechirper to the end of SASE1 is shown in Fig. 4. It can be seen that

the losses start at the dechirper location and then decrease along the beam line, however, there is a large increase of losses near the entrance of SASE1, which can be attributed to the two vacuum chamber aperture transitions at the undulator entrance. Along the undulator beam line, one can observe another two peaks around 210 m and 320 m. These two peaks might be generated by the large period betatron oscillations from the particles scattered in the dechirper.

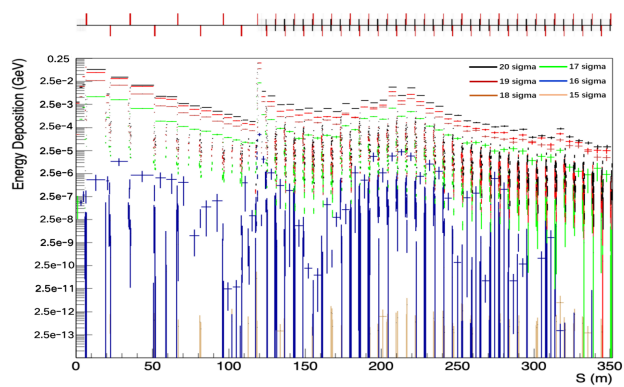


Figure 4: Energy loss per element per event from the entrance of dechirper to the end of SASE1 beam line. The horizontal error bar indicates the length of the element and the vertical error bar indicates the statistic fluctuation of the simulation.

In Fig. 4, one can also see that, the maximum energy deposition after vacuum chamber transition is at around 210 m. According to the energy deposition distribution, radiation dose map can be obtained by BDSIM Scoring [10], as shown in Fig. 5 for the case with 20 sigma halo extension.

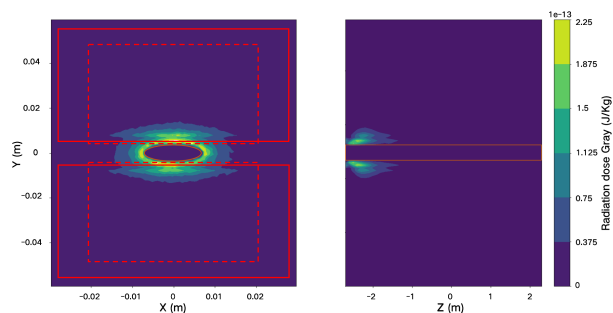


Figure 5: Example of scoring map of undulator cross-section for beam halo extension with 20 sigma. The orange ellipse indicates the elliptical undulator vacuum chamber, the red square with solid line indicates the magnet of undulator and the red square with dotted line indicates the pole of undulator.

The radiation loss generated per hour can be derived from the following equation:

$$D = R \cdot N_e \cdot F \cdot N_b \cdot T, \quad (1)$$

Content from this work may be used under the terms of the CC BY 3.0 licence (© 2021). Any distribution of this work must maintain attribution to the author(s), title of the work, publisher, and DOI

where  $R$  is the radiation dose per event (one event is one electron) in Gray,  $N_e$  is the total number of electrons in one bunch,  $F$  is the fraction of beam halo (from 10 sigma to 15-20 sigma) within one bunch<sup>1</sup>,  $N_b$  is number of bunches per second,  $T$  means one hour of machine running time and  $D$  means the radiation dose per hour.

Using Eq. (1) and the results from Fig. 5, we obtained the dose for the case of 20 sigma halo extension as  $D_{20\sigma} = 2.85$  Gray per hour for the maximum  $N_b$  of 27000 and  $N_e$  of  $1.56 \times 10^9$  (for the bunch charge of 250 pC). According to previous radiation damage studies on the European XFEL undulator system [12, 13], the maximum acceptable dose is estimated to be about 55 Gy/10 years, which means no more than 0.04% demagnetization occur in 10 years of operation. If we assume 300 hours per year for dechirper related studies, then the acceptable dose per hour  $D_{\text{acceptable per hour}}$  would be 0.0183 Gray. In order to estimate how many number of sigma is acceptable, we reduced the number of sigma from 20 sigma to 15 sigma and calculated the corresponding dose per hour, as shown in Fig. 6. From the results shown in Fig. 6, 16 sigma of beam halo extension is acceptable. However, in order to run more shifts, below 16 sigma would be optimal.

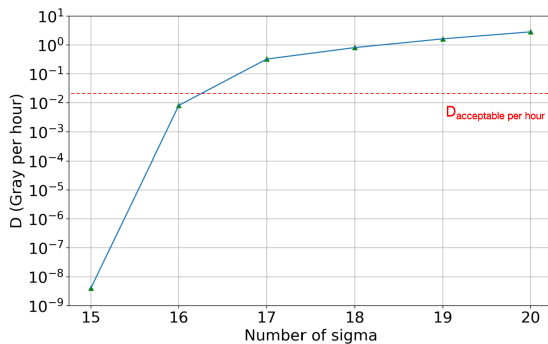


Figure 6: Radiation dose obtained from simulations with different extension of beam halo.

Please note that the above mentioned results are only valid for the vertical beam halo with the design optics. One can certainly modify the orientation of the dechirper and/or the optics to loose the constraints. For example, if two dechirper modules were installed vertically, maximum acceptable sigma of beam halo would be 32 sigma, because betafuncion and emittance in X direction (Vertical dechirper) are much smaller than in Y direction (Horizontal dechirper) (see Fig. 1 and Table 2).

## BEAM HALO MEASUREMENTS

In order to characterize the beam halo in the current operated machine, beam halo measurements have been performed using one wire scanner near the potential dechirper installation location. Measurements have been performed

<sup>1</sup> The fraction of beam halo beyond 10 sigma is estimated to be less than  $1 \times 10^{-4}$  [11, 12], here we take  $1 \times 10^{-4}$  as the worst case scenario.

with 250 pC beam charge and with  $\phi 8$  mm main collimator apertures [14]<sup>2</sup>. One example of the measured horizontal and vertical beam halo distributions with two detectors (beam loss monitors) is presented in Fig. 7, which shows that the horizontally and vertically measurable beam halo are constrained in  $30 \sigma$  and  $20 \sigma$  level, respectively. The origin of the beam halo is still under investigation. Unfortunately, it is difficult to calculate the fraction of beam halo from these measurements due to limited dynamic range of the detectors. However, as we mentioned before, a rough estimation of fraction of beam halo beyond 10 sigma would be less than  $1 \times 10^{-4}$ .

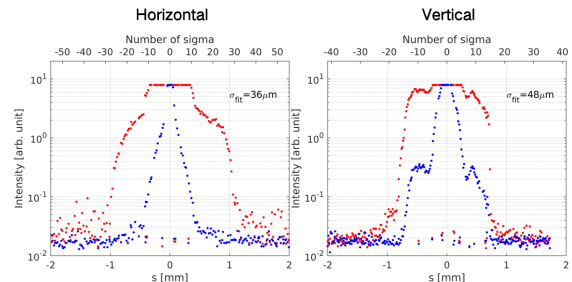


Figure 7: One example of horizontal (left) and vertical (right) beam halo distributions measured by the wire scanners upstream of SASE1. Two detectors (in blue and red) with different high voltage settings have been used for the measurements.

## DISCUSSIONS AND PROSPECTS

In this paper, beam loss simulations from 15 sigma to 20 sigma of beam halo have been performed for the case with two horizontal dechirper modules. Simulation results showed that, below 16 sigma of beam halo would be optimal for running 300 hours per year. If two dechirper modules will be installed vertically, maximum acceptable sigma of beam halo would be 32 sigma. We have also tried to extend the number of dechirper modules to three, however, in this case, we have observed even more energy deposition and radiation dose in the downstream undulators. Beam halo measurements using wire scanners have been performed near the potential dechirper installation location. Measurements will be continued to investigate the beam halo origin and intensity.

In the future, we will add additional shielding/collimation downstream of the dechirper modules in our simulation and check if they can help to reduce the doses in the undulators.

## ACKNOWLEDGEMENTS

The authors would like to thank the colleagues at DESY, especially N. Golubeva and S. Walker for fruitful discussions. And thanks to S. Boogert and L. Nevay from RHUL for their support on BDSIM.

<sup>2</sup> In normal operation,  $\phi 6$  mm apertures are usually used for the four main collimators, and the smallest apertures are  $\phi 4$  mm.

## REFERENCES

- [1] W. Decking *et al.*, “A MHz-repetition-rate hard X-ray free-electron laser driven by a superconducting linear accelerator”, *Nature Photonics*, vol. 14, no. 6, pp. 391–397, 2020. doi:10.1038/s41566-020-0607-z
- [2] J. N. Galayda, “The LCLS-II: A High Power Upgrade to the LCLS”, in *Proc. 9th Int. Particle Accelerator Conf. (IPAC’18)*, Vancouver, Canada, Apr.-May 2018, pp. 18-23. doi:10.18429/JACoW-IPAC2018-MOYGB2
- [3] Z. Zhu, Z. Zhao, D. Wang, Z. Yang, and L. Yin, “SCLF: An 8-GeV CW SCRF Linac-Based X-Ray FEL Facility in Shanghai,” in *Proc. 38th Int. Free Electron Laser Conf. (FEL’17)*, Santa Fe, NM, USA, Aug. 2017, pp. 182-184. doi:10.18429/JACoW-FEL2017-MOP055
- [4] A. A. Lutman *et al.*, “Fresh-slice multicolour X-ray free-electron lasers”, *Nature Photonics*, vol. 10, no. 11, pp. 745–750, Nov. 2016. doi:10.1038/nphoton.2016.201
- [5] C. Emma *et al.*, “Experimental demonstration of fresh bunch self-seeding in an X-ray free electron laser”, *Applied Physics Letters*, vol. 110, no. 15, p. 154101, 2017. doi:10.1063/1.4980092
- [6] A. A. Lutman *et al.*, “High-power femtosecond soft X rays from fresh-slice multistage free-electron lasers”, *Physical Review Letters*, vol. 120, p. 264801, Jun. 2018. doi:10.1103/PhysRevLett.120.264801
- [7] I. Agapov, G. Blair, S. Malton, and L. Deacon, “BDSIM:A particle tracking code for accelerator beam-line simulations including particle-matter interactions”, *Nuclear Instruments and Methods in Physics Research Section A: Accelerators, Spectrometers, Detectors and Associated Equipment*, vol. 606, no. 3, pp. 708–712, 2009. doi:10.1016/j.nima.2009.04.040
- [8] I. Zagorodnov, G. Feng, and T. Limberg, “Corrugated structure insertion for extending the sase bandwidth up to 3% at the European XFEL”, *Nuclear Instruments and Methods in Physics Research Section A: Accelerators, Spectrometers, Detectors and Associated Equipment*, vol. 837, pp. 69–79, 2016. doi:10.1016/j.nima.2016.09.001
- [9] BDSIM manual, [http://www.pp.rhul.ac.uk/bdsim/manual/model\\_control.html#halo](http://www.pp.rhul.ac.uk/bdsim/manual/model_control.html#halo)
- [10] L. J. Nevay *et al.*, “BDSIM: Recent Developments and New Features Beyond V1.0”, in *Proc. 10th Int. Particle Accelerator Conf. (IPAC’19)*, Melbourne, Australia, May 2019, pp. 3259-3262. doi:10.18429/JACoW-IPAC2019-WEPTS058
- [11] S. Liu *et al.*, “First Beam Halo Measurements Using Wire Scanners at the European XFEL”, in *Proc. 38th Int. Free Electron Laser Conf. (FEL’17)*, Santa Fe, NM, USA, Aug. 2017, pp. 255-258. doi:10.18429/JACoW-FEL2017-TUP003
- [12] S. Liu, W. Decking, and F. Wolff-Fabris, “Study of Possible Beam Losses After Post-Linac Collimation at European XFEL”, in *Proc. 9th Int. Particle Accelerator Conf. (IPAC’18)*, Vancouver, Canada, Apr.-May 2018, pp. 4092-4095. doi:10.18429/JACoW-IPAC2018-THPMF022
- [13] F. Wolff-Fabris, F. Hellberg, J. Pflüger, and F. Schmidt-Föhre, “Status of the Radiation Damage on the European XFEL Undulator Systems”, in *Proc. 9th Int. Particle Accelerator Conf. (IPAC’18)*, Vancouver, Canada, Apr.-May 2018, pp. 1776-1779. doi:10.18429/JACoW-IPAC2018-WEYGBD2
- [14] V. Balandin, R. Brinkmann, W. Decking, and N. Golubeva, “Optics solution for the xfel post-linac collimation section”, DESY, Hamburg, Germany, Rep. TESLA-FEL 2007-05, 2007.